

A Hybrid Clustering Approach: Segmentation and Classification of Brain Tumour Utilizing SVM and CNN Methods



Mahendran Kantharimuthu^{1*}, Malathi Marichamy²

¹ Department of ECE, Hindusthan Institute of Technology, Coimbatore 641032, India

² Department of EE-VLSI, Rajalakshmi Institute of Technology, Chennai 600124, India

Corresponding Author Email: dr.mahendran.k@hit.edu.in

Copyright: ©2025 The authors. This article is published by IETA and is licensed under the CC BY 4.0 license (<http://creativecommons.org/licenses/by/4.0/>).

<https://doi.org/10.18280/ts.420437>

ABSTRACT

Received: 14 December 2024

Revised: 12 April 2025

Accepted: 18 June 2025

Available online: 14 August 2025

Keywords:

magnetic resonance imaging, brain tumour, convolutional neural network, segmentation, Support Vector Machine (SVM)

Gliomas are the most prevalent and destructive kind of tumour which cause extremely short life expectancy in the highest grade. The gliomas type of tumour is assessed using medical imaging modalities like Magnetic Resonance Imaging (MRI) technique. In clinical aspects, segmentation methods need a longer time. To increase the patients' lifetime, it is necessary to perform segmentation, recognition, and removal of the affected tumour portion from the MRI images. The proposed system utilises a hybrid clustering technique called the KIFCM Technique. The complex structure, blurred boundaries, and external noise in brain tumours make MRI image segmentation essential for improving accuracy and segmentation stability. Therefore, the hybrid clustering method is proposed. The acquired MRI brain images undergo pre-processing using Otsu's thresholding, followed by hybrid clustering. Further, the segmented portions undergo feature extraction using PCA and DWT to minimise complexity and enhance the performance. The efficiency of the suggested method is compared to that of remaining frameworks for segmentation and classification. The proposed approach provides effective and quick segmentation, yielding 90% accuracy in distinguishing normal and abnormal brain MRI tissue.

1. INTRODUCTION

The important and complicated structure of the human anatomy is the brain. Billions of cells work cohesively to perform a task, making its function complex. When there is a blunt dissection of the brain cells, leading to an anomalous collection of cells inside or around the brain, it leads to brain tumour. This group of anomalous cells bothers the regular activities of the brain and abolishes the healthy tissues. The two categories of brain tumours are categorized into two types benign or low grade (Grade I & II) and malignant or high grade (Grade III & IV). Benign tumours are non-cancerous, which grows gradually and does not spread in the tissues because it is less destructive [1].

To detect the abnormalities accurately, MRI is widely recognized as a superior imaging tool that captures precise and detailed organs from inside of the body [2, 3]. The different types of MRI, like the high field MRI, which helps us capture the good images, and the low field MRI to capture low field category MRI images. MRI imaging technique helps physicians to visualize the hairline cracks and tear in muscles, certain soft tissue, and ligaments that occur during injuries. MRI is a progressive medical imaging technique that provides detailed information about human soft-tissue anatomy. In the process of automatically segmenting brain tumours, abnormal tissues can be distinguished from normal structures such as white matter (WM), gray matter (GM) and cerebrospinal fluid (CSF) [4, 5]. When comparing MRI with other methods, it

uses appropriate Radiofrequency and gradient pulses with suitable relaxation timing to produce different image components. The techniques are quite relevant to produce constant high-quality images.

The life expectancy of the tumour patients is only two years in the case of LGG and HGG glioma tumours. Several imaging techniques were utilized, such as MRI, CT, Positron emission tomography (PET), and single-photon emission tomography (SPECT). To diagnose and treat glioma, the MRI is the more proper imaging practice. Because the MRI imaging technique provides high resolution while capturing soft tissues, multi-parameter computation, arbitrary direction adjustments, noninvasive imaging, etc. Various Imaging types provide exhaustive information on images and designate the characteristics of tumour [6]. It is a challenging problem to partition the tumour portion accurately due to the shape, location, appearance, and dimensions of gliomas that can change from patient to patient. The second region is gliomas surrounded by invading tissues, making the boundary blurred. The segmentation is becoming complex due to imaging distortion due to imaging devices and the capturing methods.

2. RELATED WORK

The extensive literature relates various segmentation algorithms and classifier for extracting the tumour area from MRI brain images. The implemented method uses a

convolutional neural network [7]. The article uses preprocessing for intensity and patch normalization. The training process comprises 3*3 small kernels to acquire a feature map. Hence the feature map is coupled with a preceding layer through the kernel weights. It is tuned using the backpropagation algorithm to enhance specific input features during the training phase. The research work uses a convolutional neural network because it is easy to train CNN layers and less prone to overfitting. The described work uses a deep neural network classifier to classify a 66 brain MRI dataset into four tumour types, employing Wavelet Transform and PCA for feature extraction [8].

The author employs a modified deep convolutional neural network to categorize the abnormal tissues of the brain region. The complexity of Deep Convolutional Neural Networks (DCNNs) increases due to the greater number of layers between input and output. The computational complexity of DCNN was reduced by decreasing the number of parameters [9]. A simple assignment process helps to find the weight of this fully connected layer.

The proposed work uses fuzzy C-means and a watershed algorithm to extract tumour from MRI brain images. The algorithm employs an initial centroid selection derived from histogram calculations. The watershed algorithm uses atlas-based marker detection to eliminate over-segmentation [10]. Before performing the segmentation process, there are three fundamental processes: preprocessing to remove noise, skull removal, and contrast enhancement. Finally, the performance of these segmentation algorithms was compared.

The author offers a new technology for the early detection of brain tumours from the histopathology specimen. The segmentation of the wound from the histopathology image was difficult because of its complex nature. Convolutional Neural Network (CNN) is an innovative method to automatically perform nucleus segmentation by preserving the shape of an image. The next step was CNN modeling, which has to be performed by using features from the learned representation. Less computational time is needed to select the number of nuclei in an image and develop a method to classify the multiclass brain tumour. The author used SVM and ANN for brain tumour classification.

Texture-related features are extracted from the SROI region and a genetic algorithm is used to select the optimal features

from the dataset. DWT and Bayesian Neural Network methods are employed to classify tumours using Magnetic Resonance Spectroscopy. Removal of noise from the MRS signal is performed at the preprocessing stage using DWT. The suggested method uses a Bayesian-based neural network to classify the tumour types.

The implemented technique helps to identify the tumour in an earlier stage. The accurateness of the tumour classification is enhanced by proper selection of features, which reduces the redundancy and increases the classification efficiency [11]. The proposed technique combines the two methods, namely rough tolerance set and freely algorithm, which helps to identify the suitable features from the collection of many features like intensity, shape, and textures. Based on the appropriate feature selection, the classification is made.

The author uses the 2D-DWT. The different co-efficient are extracted using wavelet, PCA and linear discriminant study to help identify the suitable features for classification of abnormal [12]. The selected features are used by K-nearest Neighbor and SVM to categorize the abnormality. The proposed technique based on compressed sensing MRI to capture the brain images. The author proposed exponential wavelet shrinkage [13]. The implemented method provides better results than the iterative shrinkage thresholding algorithm.

Through this detailed review, it is understood that K-means and fuzzy cmeans were the conventional algorithms to segment the tumour portion for the MRI brain image. K-means algorithms perform poorly in segmentation with noise and artifacts, whereas Fuzzy C-means segmentation, offering more valuable information for detecting malignant tumours, entails a longer processing time. Hence, the proposed research work implements a new methodology called hybrid clustering using MATLAB. The disadvantages of above above-discussed algorithm have been overcome by merging the above two algorithm, called hybrid clustering is used for our research work. Next, the segmentation portion is classified as normal or abnormal. It has been implemented using CNN and SVM.

The following Table 1 presents an overview of the ablation study which incorporates K-means, KIFCM, and FCM. KIFCM outperforms FCM and K-means in terms of noise presence, blurred boundary preservation, and tumor segmentation boundary delineation.

Table 1. Comparison of K-means, FCM and KIFCM

S. No.	Method	Accuracy (%)	PSNR (dB)	MSE	Noise Handling	Boundary Preservation	Computation Time (secs)
1	K-means	70	21.618	447.9185	Poor	Moderate	5.1513
2	FCM	80	21.186	494.7511	Moderate	Good	5.3962
3	KIFCM	80	21.186	494.7511	Excellent	Excellent	5.1511

3. RESEARCH METHODOLOGY

The brain tumour is in different sizes and shapes; it is hard to perform segmentation because MRI images have information at multiple scales due to their broader structure. Hence, to capture the information at various levels, decomposition of the images into different frequency bands was done using DWT. MRI images are a huge dimensional dataset; hence, it takes more values to represent the voxel in the spatial dimension. Dimensionality reduction using DWT-based PCA reduces the computation time further and helps to avoid overfitting. It is more effective in denoising MRI images, which enhances the robustness of feature extraction.

The proposed model uses multiscale feature extraction, dimensionality reduction, noise robustness, and hybrid clustering to capture subtle variations in tissue characterization, allowing for more accurate segmentation results.

The proposed methodology uses a CNN and SVM-based architecture to identify the tumour from an MRI brain image. The implemented technique comprises the following steps for brain tumour classification. The suggested work is depicted in the overview provided in Figure 1.

Step 1: Data set collection and preprocessing.

Step 2: Segmentation of tumour is achieved by hybrid clustering.

Step 3: Utilize DWT and PCA for feature extraction to reduce dimensionality.

Step 4: CNN and SVM based classification and analyse the performance of the two classifiers.

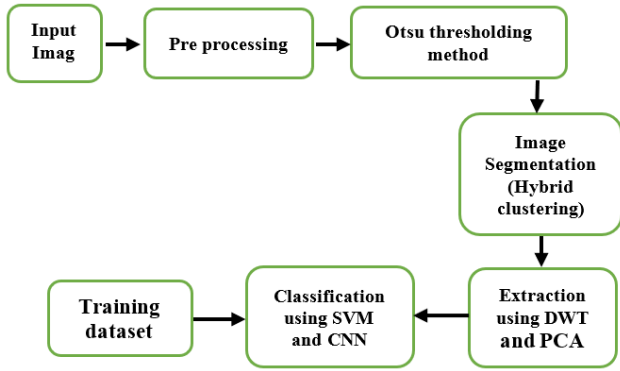


Figure 1. Process flow diagram

3.1 Data set and preprocessing

The 2020 BRATS training dataset contains 399 multi-modality MRI scans, including 293 from glioblastoma (GBM/HGG) and 76 from lower grade glioma (LGG), along with their respective ground truth segmentations for evaluation.

The image size is 512×512 pixels with a dimension of 0.49×0.49 mm². Data augmentation and random transformations are used to reduce overfitting of the neural network in the training phase. 80% used for training, while the rest 20% for testing. The data augmentation technique is employed to provide robustness, preserve spatial features from MRI brain images, and increase the precision and reliability of the detection process. Rotating operations is a common data augmentation technique used in brain tumour segmentation. Rotating operations are applied to the input images during each epoch of training. It helps the CNN model learn features that are relevant to such transformations. Additional training samples are generated using random flipping along with the original dataset. The CNN and SVM models are trained using the augmented dataset, which helps the models become more robust and reduce overfitting. Additionally, it helps to increase the generalization capabilities of the CNN and SVM models. Dropout layers are used before the fully connected layer to reduce overfitting.

With respect to the class imbalance present in the BRATS dataset, which has a significantly higher number of HGG cases than LGG cases (293 vs. 76), we covered this gap with strong data augmentation, like rotating and flipping to increase the amount of LGG samples in the training set. With the application of these augmentations in dynamic epochs, the model was able to further improve generalization, mitigating overfitting. While we did not actively apply weighting loss functions or oversampling, the augmenting approach provided passive albeit effectively balanced, inputs. For class imbalance with the aim of reinforcing segmentation performance in both types of tumors, further methods like class-weighted loss and synthetic over-sampling (e.g., SMOTE) will be explored in later work.

3.2 Image binarization

Binarization, a fundamental image processing step, involves

converting a grayscale image into a binary image. The two possible values for each pixel, often zero and one as in the equation, are called a binary image (I) ($I : (x, y) \rightarrow (0,1)$). Binarization refers to the fundamental process within an image that helps separate the foreground object from the background, as shown in Figure 2.

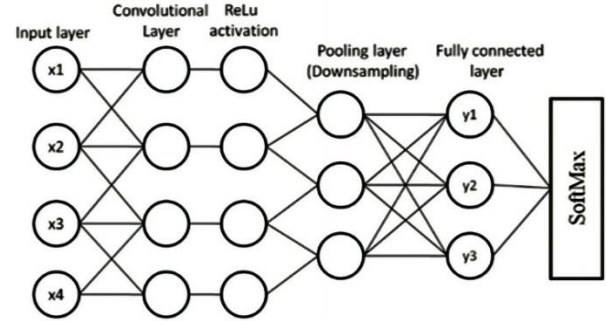


Figure 2. Convolutional neural network

The proposed research work uses Otsu's based thresholding method. The main goal of this method is to find the optimal threshold value.

This approach involves grouping pixels into two corresponding classes, C1 and C2, based on a bimodal histogram, aiming to select thresholds that minimize intraclass variance using a weighted equation for each cluster.

$$\sigma^2 w(t) = q_1(t) \sigma_1^2(t) + q_2(t) \sigma_2^2(t) \quad (1)$$

where,

The weight q_i is the probability for each class.

It can be considered as follows

$$\begin{aligned} q_1(t) &= \sum_{i=1}^t P_i \\ q_2(t) &= \sum_{i=t+1}^l P_i \\ \mu_1(t) &= \sum_{i=1}^t \frac{iP(i)}{q_1(t)} \\ \mu_2(t) &= \sum_{i=t+1}^l \frac{iP(i)}{q_2(t)} \end{aligned}$$

The distinct class variance is specified by

$$\begin{aligned} \sigma_1^2(t) &= \sum_{i=1}^t [i - \mu_1(t)]^2 \frac{P_i}{q_1(t)} \\ \sigma_2^2(t) &= \sum_{i=t+1}^l [i - \mu_2(t)]^2 \frac{P_i}{q_2(t)} \end{aligned}$$

After the variance is computed, the procedure is terminated

$$\sigma_b^2(t) = \sigma - \sigma_w^2(t) = q_1(t) - q_2(t)[\mu_1(t) - \mu_2(t)]^2 \quad (2)$$

The technique is employed to minimize intra-class variance while maximizing between-class variance.

3.3 Image segmentation

The process of dividing the entire image into smaller regions is called segmentation. It is necessary to segment the features in an image since distinct features require focus and clustering falls under simple unsupervised learning. Grouping of pixels with similar intensity is known as clustering, which is done without any training images. Hybrid segmentation refers to the process of integrating two segmentation algorithms.

The purpose of combining various algorithms is to eliminate the shortcomings of two dissimilar methods and to improve the good segmentation results. The result is shown in the Figure 3. The combination of fuzzy C-means with K-means is called the KIFCM technique, which is used for accurate tumour detection from MRI images [14]. By integrating Fuzzy C-Means and K-Means, the KIFCM technique improves tumor detection accuracy in MRI images due to the shortcomings of each method. It increases segmentation precision and decreases computational time. Careful segmentation design considerations are necessary to ensure quality segmentation results.

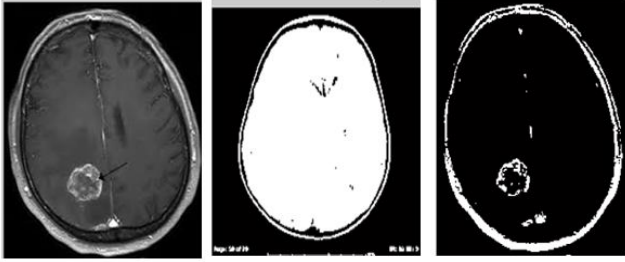


Figure 3. Segmentation results (a) Input image (b) Otsu's threshold image (c) Segmentation of tumour

3.4 Feature extraction

The computational complexity of processing large dataset was reduced by feature reduction.

The extracted features, including intensity and texture-based ones such as contrast, energy, and entropy, aid in classifying MRI brain images into dissimilar regions like GM, WM, CSF, and tumour.

3.5 Discrete wavelet transform

The different frequencies of an image were analyzed with the help of a wavelet. DWT is one of the tools for feature extraction. Wavelet helps in localizing frequency information important for classification, with spatial frequency components acquired from LL and HL sub-bands, which describe image texture features. The statistical features are obtained using gray level co-occurrences matrix (GLCM). The statistical features are obtained using GLCM and also gray-level spatial dependence matrix (GLSDM). The proposed research work uses GLCM to extract features like contrast; correlation, energy, homogeneity, entropy, and variance were obtained from LL and HL sub bands of the first four levels of wavelet decomposition.

3.6 Principal component analysis

The main use of PCA is dimensionality reduction. Feature extraction can be performed on both the training MR image and testing MR image. During testing and training phase, feature extraction can be done. During the training phase, the features are removed from each training MR image [15]. The training image 1 can be represented by and the pixel resulting is $M \times N$ (M rows and N columns).

The PCA algorithm reduces the dimensionality of feature vectors for both training and test images. It computes the Euclidean distance similarities among the reduced feature vectors of test and training images for classification.

The MRI image [16] is correctly classified if $i = j$; otherwise,

i it is misclassified.

MRI images are multiscale, and they hold information that can be retrieved by DWT in frequency bands as images are decomposed. Because of the high dimensionality of MRI data, computation time, overfitting, and noise, PCA is employed post-DWT to enhance these attributes. Although DWT ensures the frequency components that are non-linear and relevant to the tumor are preserved, which is why PCA isn't a problem. Then DWT ensures that the most informative features based on variance are retained. Unlike t-SNE or Autoencoders, PCA does not require training, works well with DWT, is more efficient, and is not time-consuming. This leads to the preservation of vital tumor characteristics, which leads to improved segmentation accuracy.

4. RESULTS AND DISCUSSION

4.1 Convolutional neural network

The suggested approach goes through the MRI brain image, one pixel at a time, using a sliding window that covers the whole image. Each pixel gets classified based on its surrounding $N \times N$ neighborhood, and then it's fed into a CNN architecture. The implementation model selects kernel sizes of $11 \times 11 \times 7$ and 3×3 pixels, respectively, and a window of 65×65 pixels. Each pathway utilizes 3×3 max-pooling kernel with a stride of 3 and two convolutional layers with ReLU activation. The large, medium, and tiny pathways generate 128, 96, and 64 feature maps, respectively. Window features are obtained by employing numerous maps at various scales, distinguishing three tumour types [17] for classification. Concatenation is performed on a scale features in a convolutional layer using a 3×3 kernel and ReLU activation, followed by 2×2 max-pooling kernel operation with a stride of 2. Subsequently, the concatenated features are given into a fully connected stage for classification, incorporating dropout layers to mitigate overfitting and utilizing SoftMax activation in the final layer [18].

4.2 Initialization

Xavier initialization helps to obtain convergence. It also helps to maintain the activation, and the gradients are retained in controlled levels, then the back-propagated gradients help to disappear or explore.

4.3 Activation function

It can change the data rectifier linear units (ReLU), defined as $F(x) = \max(0, x)$. The ReLU helps to obtain better outcomes than conventional activation functions like sigmoid or hyperbolic tangent functions. The introduction of a constant 0 can improve the gradient flow and subsequent adjustments of weights. These restrictions can be overcome using a variant called Leaky rectifier linear unit (LReLU), which is capable of providing an insignificant slope on the negative part of the function.

$$F(x) = \max(0, x) + \alpha \min(0, x) \quad (3)$$

Here, α is the leakiness parameter we use softmax in the last FC layer. Max pooling helps reduce the computational load of each stage by aggregating spatial features within the feature maps.

4.4 Regularization

The overfitting in CNN [19, 20] can be reduced with the help of regularization. The FC layer uses dropout, which helps to remove node with probability of P in the network. It also used in various networks and produces a form of bagging, because every network has been trained with a portion of the training data.

4.5 Data enrichment

To reduce overfitting and enhance the generalization performance on unseen data, it is crucial to integrate augmentation and normalization techniques into the pre-processing of MRI brain tumour segmentation. This integration enhances the reliability and accuracy of segmentation. The normalization process standardizes the pixel intensities across MRI images with techniques such as Z-score regularization or min-max scaling. This standardization ensures that the range of values is consistent across various images. Consistent pixel values help maintain the stability of the training process by preventing extreme pixel values from dominating the optimization process. This, in turn, provides more stable convergence during training. Data augmentation increases the dataset by creating modified versions of existing images using rotations. By exposing the model to a larger range of variations present in MRI images, augmentation helps prevent the model from memorizing specific patterns during training. Instead, the model learns to identify essential features across augmented samples, reducing its susceptibility to overfitting. Overall, integrating normalization and augmentation techniques into pre-processing significantly improves the reliability and accuracy of MRI brain tumour segmentation by enhancing generalization performance on unseen data.

4.6 SVM classifier

SVM is a good classifier for image recognition, function approximation, and data classification. Various linear and nonlinear architectures, such as linear discriminant analysis, multi-layer perceptrons, K nearest neighbours, and least square minimum distance (LMSD), have been developed to classify abnormal portions of an image. SVM offers the best classification result out of all those nonlinear classifiers. Two fundamental procedures are involved in SVM classification: testing and training.

A SVM locates the optimal unscrambling hyperplane amidst members of a specific class within a high-dimensional feature space.

$$K(x_i, x_j) = (x_i^T x_j + 1)^p \geq 0 \quad (4)$$

One of the simplest SVM is linear SVM, in which the output patterns are linearly discernible. It can be expressed by

$$F(X) = W^T + bx \quad (5)$$

In the linear case, every training sample X_i provides the output function

$$Y_i = \pm 1 \text{ for } f(x_i) \geq 0 \text{ and } Y_i = 1 \text{ for } f(x_i) \leq 0 \quad (6)$$

Due to that the hyperplane separates the two different classes of samples

$$F(x) = W^T + bx \quad (7)$$

After the completion of the segmentation process, it is essential to classify the segmented image using classifiers such as SVM and CNN. SVM is a linear classifier that is mostly used in classification problems. Unlike SVM, CNN is nonlinear and is most suitable for visual image recognition. The following Tables 1 and 2 provide various lists of extracted features for non-cancerous and cancerous brains.

C*-Contrast; C-Correlation; E*-Energy; H-Homogeneity; M-Mean; SD-Standard Deviation; E-Entropy; V-Variance; R-RMS; S-Smoothness; S*-Skewness; K-Kurtosis.

Images of the brain tumour at each step are shown, and a comparative relation of the classifier SVM and CNN is performed with the parameters: accuracy, time, PSNR and MSE. The SVM classifier produced the best result compared to the CNN classifier.

The features extracted for benign and malignant MRI brain tumour. This is shown in Tables 2 and 3, which help to analyze each and every feature of cancerous and non-cancerous cells in an effective way. Before the classification of the brain cells it is necessary to identify the texture of abnormal portions. The proposed work uses CNN and an SVM classifier to analyze the abnormal portions. For which it is compulsory to train the network by giving large number of data sets. Once the system is trained properly, we need to check whether the test data is normal or abnormal. Table 4 compares the two classifiers in terms of accuracy, time, PSNR, and MSE.

Table 2. Benign tumour images with the values of parameters extracted using feature extraction

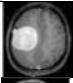
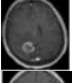
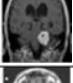
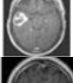
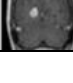
S. No	Input Image	C*	C	E *	H	M	SD	E	R	V	S	S*	K
1.		0.208	0.199	0.762	0.935	0.03	0.089	3.173	0.893	0.008	0.920	0.469	7.328
2.		0.271	0.093	0.768	0.933	0.02	0.089	3.269	0.089	0.008	0.897	0.886	7.956
3.		0.244	0.100	0.740	0.926	0.003	0.089	3.579	0.089	0.008	0.923	0.633	6.273
4.		0.216	0.138	0.754	0.932	0.002	0.089	3.315	0.089	0.008	0.903	0.312	6.232
5.		0.225	0.099	0.769	0.936	0.002	0.089	3.518	0.089	0.008	0.885	0.441	6.767

Table 3. Malignant tumour images with the values of parameters extracted using feature extraction

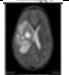
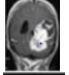
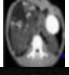
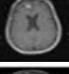
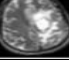
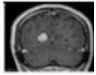
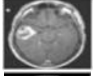
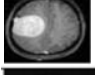
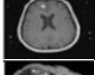
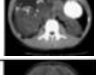
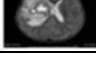
S. No	Input Image	C*	C	E *	H	M	SD	E	R	V	S	S*	K
1.		0.305	0.142	0.786	0.937	0.006	0.089	3.205	0.089	0.008	0.959	1.104	12.240
2.		0.227	0.132	0.743	0.929	0.004	0.089	3.604	0.089	0.008	0.940	0.521	5.997
3.		0.243	0.093	0.761	0.932	0.003	0.089	3.371	0.089	0.008	0.931	0.635	7.350
4.		0.265	0.132	0.767	0.934	0.004	0.089	3.063	0.089	0.008	0.944	0.953	12.168
5.		0.243	0.107	0.731	0.924	0.004	0.089	3.548	0.089	0.008	0.944	0.620	6.523

Table 4. Performance analysis table

S. No	Types of Tumour	Image	Classifier	Accuracy In %	PSNR (db)	MSE (No.of bits/pixel)	Time (secs)
1.	Benign		SVM	70	21.618	447.9185	5.1513
			CNN	60	21.584	451.4868	16.645
2.	Benign		SVM	60	22.145	396.7803	5.1700
			CNN	40	22.001	384.6298	16.622
3.	Benign		SVM	50	21.368	474.4520	13.510
			CNN	30	21.220	470.2738	19.990
4.	Malignant		SVM	80	21.186	494.7511	5.3962
			CNN	50	21.387	472.4432	16.674
5.	Malignant		SVM	70	21.370	474.3339	5.1511
			CNN	40	21.209	492.2409	16.599
6.	Malignant		SVM	60	21.125	501.7942	5.2337
			CNN	60	20.880	530.9734	16.701

In this study, SVM was implemented with GLCM features while training CNN with raw MRI images. This disparity in representation affects performance, considering GLCM as structured input templates gives an advantage to SVM. Given the behavior intended to be demonstrated with these model configurations. In future work, the work aims to carry out an ablation study where both SVM and CNN are assessed under the same feature extraction methodology, be it raw pixels being used or GLCM, to more rigorously validate the performance differences between the two.

To understand the impact of performance distinction between SVM and CNN, we analyzed the accuracy, PSNR, and MSE values through paired t-tests. The results proved that SVM had a statistically significant improvement in accuracy compared to CNN ($p = 0.0121$). However, the differences in PSNR ($p = 0.2257$) and MSE ($p = 0.8075$) metrics were not statistically significant. This suggests that SVM having better accuracy is most probably not because of chance.

5. VALIDATION

The research work compares MRI brain tumour segmentation using various methods such as Random Forest, Decision Tree, U-Net, and Seg-Net. The performance of segmentation relies on handcrafted features like intensity and texture features. However, SVM struggles with capturing complex spatial relationships and variations in MRI brain

images compared to deep learning methods. Random Forest, along with other segmentation processes, provides ensemble learning approaches that build multiple decision trees during training, yet it faces challenges in capturing spatial dependencies effectively. Decision Tree, when employed for MRI brain tumour segmentation with a single tree, struggles to capture complex patterns. Another well-known deep learning architecture is U-Net, which has a symmetric expanding path for accurate localization and a controlling path to capture context.

The skip connections of the U-Net help retain high-resolution features, resulting in superior performance compared to conventional CNNs, albeit achieved with a smaller dataset. Comparatively, CNN-based methods for MRI brain tumour segmentation require larger datasets. However, the SVM method outperforms with fewer datasets. The choice of the method depends on various factors such as computational resources, data availability, and the specific requirements of the segmentation task. The proposed research work used in BRATS 2020 dataset. The SVM model outperforms for smaller datasets with less computational power and provides clear decision boundaries. However, the CNN model requires a larger dataset for training and higher computational resources. The practical deployment aspects are very important. Steps taken to increase performance allowed us to add a discussion on the model interpretability issues (particularly with SVMs) and propose later using XAI approaches, like SHAP, to support trust by clinicians. On the

other hand, our system demonstrates low-latency inference on mid-level GPUs, thus, real-time segmentation is achievable. Figure 4 shows a bar chart.

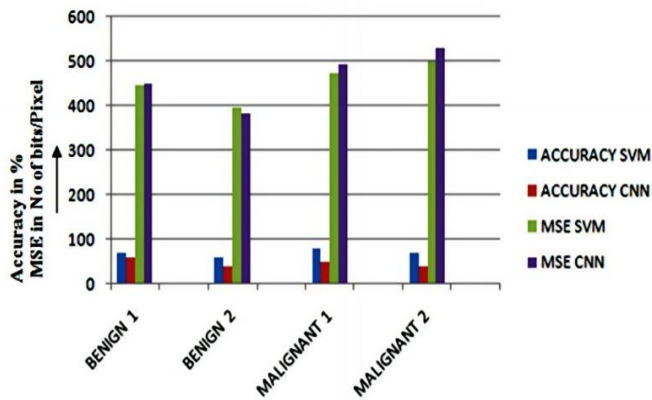


Figure 4. Bar chart

6. CONCLUSION

The computed result provides the segmented image of a brain tumour and identifies the type of tumour. Identifying tumours is verified with the patient scan image, which produces the same result as per doctor diagnosis. The classifiers (SVM and CNN) are compared with the following parameters: accuracy, PSNR, MSE, and time. SVM classifier produces high accuracy and gets executed in short period when compared to CNN classifier. Thus, CNN is nonlinear, whereas

SVM functions as a linear classifier, while CNN excels with large datasets, contrasting SVM's widespread use in classification tasks. While CNN enhances model complexity through additional layers, SVM cannot achieve the same level of complexity. Additionally, CNN exhibits slower training speeds with large datasets. The SVM classifier is optimal for classifying brain tumours in smaller datasets, requiring less execution time. As a linear classifier with lower model complexity, it is well-suited for such tasks. The proposed research work achieves a commendable accuracy of approximately 90% on the BRATS 2020 dataset. As compared to more recent benchmarks, Vision Transformers (ViTs) have a marked improvement over traditional CNNs and SVMs since they outperform them in accuracy as they capture long range dependencies more efficiently. Notably, the computational power demand of ViTs leads to increased inference times, restricting their use in real-time medical contexts. Similarly, nnU-Net provides highly accurate segmentation but takes longer to process. In comparison, our model (SVM) retains a competitive accuracy while maintaining significantly lower computational cost, making it more appropriate for real-time, clinical environments.

ACKNOWLEDGMENTS

The authors are thankful to the reviewers for their insightful feedback and the invaluable suggestions to improve the initial version of this manuscript. The authors also thank the anonymous assistant for their help with performing the statistical analysis.

REFERENCES

- [1] Yang, A., Yang, X., Wu, W., Liu, H., Zhuansun, Y. (2019). Research on feature extraction of tumor image based on convolutional neural network. *IEEE Access*, 7: 24204-24213. <https://doi.org/10.1109/ACCESS.2019.2897131>
- [2] Wang, G., Zuluaga, M.A., Li, W., Pratt, R., Patel, P.A., Aertsen, M., Vercauteren, T. (2018). DeepIGeoS: A deep interactive geodesic framework for medical image segmentation. *IEEE Transactions on Pattern Analysis and Machine Intelligence*, 41(7): 1559-1572. <https://doi.org/10.1109/TPAMI.2018.2840695>
- [3] Wang, G., Li, W., Zuluaga, M.A., Pratt, R., Patel, P.A., Aertsen, M., Vercauteren, T. (2018). Interactive medical image segmentation using deep learning with image-specific fine tuning. *IEEE Transactions on Medical Imaging*, 37(7): 1562-1573. <https://doi.org/10.1109/TMI.2018.2791721>
- [4] Razzak, M.I., Imran, M. Xu, G. (2019). Efficient brain tumor segmentation with multiscale two-pathway-group conventional neural networks. *IEEE Journal of Biomedical and Health Informatics*, 23(5): 1911-1919. <https://doi.org/10.1109/JBHI.2018.2874033>
- [5] Xing, F., Xie, Y., Yang, L. (2015). An automatic learning-based framework for robust nucleus segmentation. *IEEE Transactions on Medical Imaging*, 35(2): 550-566. <https://doi.org/10.1109/TMI.2015.2481436>
- [6] Greenspan, H., Ruf, A., Goldberger, J. (2006). Constrained Gaussian mixture model framework for automatic segmentation of MR brain images. *IEEE Transactions on Medical Imaging*, 25(9): 1233-1245. <https://doi.org/10.1109/TMI.2006.880668>
- [7] Pereira, S., Pinto, A., Alves, V., Silva, C.A. (2016). Brain tumor segmentation using convolutional neural networks in MRI images. *IEEE Transactions on Medical Imaging*, 35(5): 1240-1251. <https://doi.org/10.1109/TMI.2016.2538465>
- [8] Mohsen, H., El-Dahshan, E.S.A., El-Horbaty, E.S.M., Salem, A.B.M. (2018). Classification using deep learning neural networks for brain tumors. *Future Computing and Informatics Journal*, 3(1): 68-71. <https://doi.org/10.1016/j.fcij.2017.12.001>
- [9] Özyurt, F., Sert, E., Avcı, D. (2020). An expert system for brain tumor detection: Fuzzy C-means with super resolution and convolutional neural network with extreme learning machine. *Medical Hypotheses*, 134: 109433. <https://doi.org/10.1016/j.mehy.2019.109433>
- [10] Benson, C.C., Deepa, V., Lajish, V.L., Rajamani, K. (2016). Brain tumor segmentation from MR brain images using improved fuzzy c-means clustering and watershed algorithm. In *2016 International Conference on Advances in Computing, Communications and Informatics (ICACCI)*, Jaipur, India, pp. 187-192. <https://doi.org/10.1109/ICACCI.2016.7732045>
- [11] Jothi, G. (2016). Hybrid Tolerance Rough Set–Firefly based supervised feature selection for MRI brain tumor image classification. *Applied Soft Computing*, 46: 639-651. <https://doi.org/10.1016/j.asoc.2016.03.014>
- [12] Kalbkhani, H., Shayesteh, M.G., Zali-Vargahan, B. (2013). Robust algorithm for brain magnetic resonance image (MRI) classification based on GARCH variances series. *Biomedical Signal Processing and Control*, 8(6):

- 909-919. <https://doi.org/10.1016/j.bspc.2013.09.001>
- [13] Zhang, Y., Dong, Z., Phillips, P., Wang, S., Ji, G., Yang, J. (2015). Exponential wavelet iterative shrinkage thresholding algorithm for compressed sensing magnetic resonance imaging. *Information Sciences*, 322: 115-132. <https://doi.org/10.1016/j.ins.2015.06.017>
- [14] Özyurt, F., Sert, E., Avcı, D. (2020). An expert system for brain tumor detection: Fuzzy C-means with super resolution and convolutional neural network with extreme learning machine. *Medical Hypotheses*, 134: 109433. <https://doi.org/10.1016/j.mehy.2019.109433>
- [15] Zhang, Y., Dong, Z., Phillips, P., Wang, S., Ji, G., Yang, J. (2015). Exponential wavelet iterative shrinkage thresholding algorithm for compressed sensing magnetic resonance imaging. *Information Sciences*, 322: 115-132. <https://doi.org/10.1016/j.ins.2015.06.017>
- [16] Eali, S.N.J., Bhattacharyya, D., Nakka, T.R., Hong, S. P. (2022). A novel approach in bio-medical image segmentation for analyzing brain cancer images with U-NET semantic segmentation and TPLD models using SVM. *Traitement Du Signal*, 39(2): 419-430. <https://doi.org/10.18280/ts.390203>
- [17] Kareem, N.A. (2024). A hybrid machine learning and deep learning approach for brain tumor segmentation and disease type prediction. *Journal Européen des Systèmes Automatisés*, 57(6): 1573-1582. <https://doi.org/10.18280/jesa.570604>
- [18] Zouaoui, H., Attia, A., Moussaoui, A., Akhtar, Z. (2025). A robust MR image segmentation method for enhanced brain tumor detection. *Ingénierie des Systèmes d'Information*, 30(4): 1077-1085. <https://doi.org/10.18280/isi.300423>
- [19] Kantharimuthu, M., Malathi, M., Sinthia, P. (2023). Oral cancer prediction using a probability neural network (PNN). *Asian Pacific Journal of Cancer Prevention: APJCP*, 24(9): 2991. <https://doi.org/10.31557/APJCP.2023.24.9.2991>
- [20] Vankayalapati, R., Muddana, A.L. (2021). Denoising of images using deep convolutional autoencoders for brain tumor classification. *Revue d'Intelligence Artificielle*, 35(6): 489-496. <https://doi.org/10.18280/ria.350607>

NOMENCLATURE

MRI	Magnetic Resonance Imaging
SVM	Support Vector Machine
CNN	Convolutional Neural Network
PET	Positron emission tomography
SPECT	Single Photon Emission Tomography
FLAIR	Fluid Attenuated Inversion Recovery
GM	Gray matter
WM	White Matter
CSF	Cerebrospinal fluid
DCNN	Deep Convolutional Neural Network
ANN	Artificial Neural network
DWT	Discrete Wavelet Transform
MRS	Magnetic Resonance Spectroscopy
PCA	Principal Component Analysis
KIFCM	K- means Integrated with Fuzzy C means
GLCM	Gray level co-occurrences matrix
GLSDM	Gray level Spatial Dependence matrix
LMSD	Least Square Minimum Distance
PSNR	Peak signal to Noise Ratio
MSE	Mean square Error